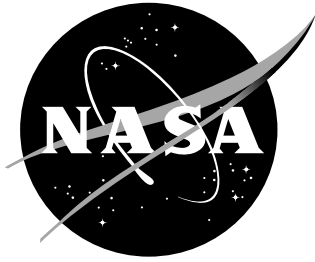# Thermal Vacuum Facility for Testing Thermal Protection Systems

Kamran Daryabeigi, Jeffrey R. Knutson, and Joseph G. Sikora
Langley Research Center, Hampton, Virginia

The NASA STI Program Office ... in Profile

Since its founding, NASA has been dedicated to the advancement of aeronautics and space science. The NASA Scientific and Technical Information (STI) Program Office plays a key part in helping NASA maintain this important role.

The NASA STI Program Office is operated by Langley Research Center, the lead center for NASA's scientific and technical information. The NASA STI Program Office provides access to the NASA STI Database, the largest collection of aeronautical and space science STI in the world. The Program Office is also NASA's institutional mechanism for disseminating the results of its research and development activities. These results are published by NASA in the NASA STI Report Series, which includes the following report types:

- TECHNICAL PUBLICATION. Reports of completed research or a major significant phase of research that present the results of NASA programs and include extensive data or theoretical analysis. Includes compilations of significant scientific and technical data and information deemed to be of continuing reference value. NASA counterpart of peer-reviewed formal professional papers, but having less stringent limitations on manuscript length and extent of graphic presentations.

- TECHNICAL MEMORANDUM. Scientific and technical findings that are preliminary or of specialized interest, e.g., quick release reports, working papers, and bibliographies that contain minimal annotation. Does not contain extensive analysis.

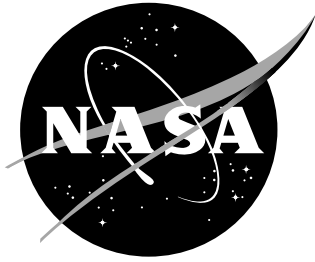- CONTRACTOR REPORT. Scientific and technical findings by NASA-sponsored contractors and grantees.

- CONFERENCE PUBLICATION. Collected papers from scientific and technical conferences, symposia, seminars, or other meetings sponsored or co-sponsored by NASA.

- SPECIAL PUBLICATION. Scientific, technical, or historical information from NASA programs, projects, and missions, often concerned with subjects having substantial public interest.

- TECHNICAL TRANSLATION. English-language translations of foreign scientific and technical material pertinent to NASA's mission.

Specialized services that complement the STI Program Office's diverse offerings include creating custom thesauri, building customized databases, organizing and publishing research results ... even providing videos.

For more information about the NASA STI Program Office, see the following:

- Access the NASA STI Program Home Page at *http://www.sti.nasa.gov*

- E-mail your question via the Internet to help@sti.nasa.gov

- Fax your question to the NASA STI Help Desk at (301) 621-0134

- Phone the NASA STI Help Desk at (301) 621-0390

- Write to:
  NASA STI Help Desk
  NASA Center for AeroSpace Information
  7121 Standard Drive
  Hanover, MD 21076-1320

Thermal Vacuum Facility for Testing Thermal Protection Systems

Kamran Daryabeigi, Jeffrey R. Knutson, and Joseph G. Sikora
Langley Research Center, Hampton, Virginia

Summary

A thermal vacuum facility for testing launch vehicle thermal protection systems by subjecting them to transient thermal conditions simulating re-entry aerodynamic heating is described. Re-entry heating is simulated by controlling the test specimen surface temperature and the environmental pressure in the chamber. The facility can be used for testing specimens as large as 18 ´ 36 in. Design requirements for simulating re-entry conditions are briefly described. A description of the thermal vacuum facility, the quartz lamp array and the control system is provided. The facility was evaluated by subjecting an 18 ´ 36 in. Inconel honeycomb panel to a typical re-entry pressure and surface temperature profile. The Inconel panel was instrumented with 23 metal-sheathed thermocouples to investigate temperature uniformity throughout the test. For most of the test duration, the average difference between the measured and desired pressures was 1.6 % of reading with a standard deviation of ±7.4%, while the average difference between measured and desired temperatures was 7.6% of reading with a standard deviation of ±6.5%. The temperature non-uniformity across the panel was 12% during the initial heating phase (t £500 sec.), and less than 2% during the remainder of the test.

List of Symbols

h	convective heat transfer coefficient
L	insulation thickness below structure backside
q''	heat flux
P	pressure
T	temperature
t	time
ΔT	temperature difference
ε	emittance
σ	Stefan-Boltzmann constant
σ_s	standard deviation

Subscripts
a	average
aw	adiabatic wall
r	radiation equilibrium

Introduction

The overall goal in thermal protection system (TPS) development is to design a TPS with the lowest possible mass that will prevent the vehicle structural temperature from exceeding a specified temperature during re-entry aerodynamic heating. A thermal protection system's overall thermal performance is evaluated by subjecting the TPS to the heating conditions and pressure environments that the system will experience during an actual re-entry. Usually a multi-panel TPS array is tested to study the overall thermal performance of the panels and the gap between panels. Testing is typically conducted in a thermal vacuum chamber where the TPS is radiantly heated, while the static pressure in the chamber is varied according to the static pressure variations during re-entry. The exact simulation of re-entry heating and pressure profiles may not be possible in a thermal vacuum facility. In this case,

experimentally imposed profiles can be used to validate computational tools for modeling heat transfer through the entire thermal protection system, and then the validated computational tool can be used to determine the overall system response to the actual re-entry profiles.

The purpose of this investigation was to develop a thermal vacuum testing facility large enough to accommodate a multi-panel TPS array, but specifically a two-panel array of the Advanced Metallic Thermal Protection System developed at NASA Langley Research Center,[1] consisting of two 18×18 in. by 3.5 in. thick panels. The overall performance of the system was evaluated by comparing the achieved surface temperature and pressure profiles with the desired re-entry profiles, and by investigating surface temperature uniformity over a simulated test article.

Design Requirements

A schematic of a typical metallic TPS is provided in Figure 1. The hot side of the system is defined as the surface of the TPS directly exposed to the aerodynamic heating during re-entry, such as the outer honeycomb panel shown in the figure. The back side is defined as the primary structure of the vehicle to which the TPS is attached. The main purpose of the TPS is to limit the temperature rise on the back side to a design limit while the hot side is exposed to the re-entry aerodynamic heating. The re-entry aerodynamic conditions and their simulation in a thermal vacuum facility are described. The TPS hot side temperature uniformity and the TPS back side thermal boundary condition are discussed.

Pressure and Heating Profiles

Simulating the exact aerodynamic heating conditions would require imposing the transient convective heating while varying the static pressure to simulate the pressure profile during re-entry. Producing these conditions in a ground test facility is very difficult. The best alternative for testing TPS is conducting thermal-vacuum tests; re-entry static pressure variation can be simulated easily, and radiant heating can be used to impose a transient temperature boundary condition that duplicates the surface temperatures that would be attained in flight under radiation equilibrium conditions. The radiative equilibrium condition assumes that the structure has reached a state so that all of the incoming aerodynamic heating is radiated from the surface of the structure to deep space at zero Kelvin:[2]

$$q'' = h\left(T_{aw} - T_r\right) = \varepsilon \sigma T_r^4 \tag{1}$$

where q'' is the heat flux, h is the convective heat transfer coefficient, T_{aw} is the adiabatic wall temperature, T_r is the radiation equilibrium temperature, ε is surface emittance, and σ is the Stefan-Boltzmann constant. Therefore, with the knowledge of the convective heating conditions, the transient radiation equilibrium temperature calculated from the above formula can be used as the imposed boundary condition to simulate the aerodynamic re-entry heating. Blosser[3] has numerically investigated the effect of imposing convective flux, radiative flux and radiation equilibrium temperature boundary conditions on the overall TPS thermal performance, and has found that the different boundary conditions produced similar results. Typical variations of radiative equilibrium temperature and static pressure, plotted as a function of elapsed time from the moment the vehicle experiences aerodynamic heating upon re-entry, are shown in Figures 2 and 3. These profiles are typical of points on vehicles that are designed to utilize a metallic thermal protection system having an 1800°F maximum operating temperature. The surface temperature rises rapidly from room temperature to 1800°F in about 500 seconds, stays at around 1800°F for almost 1000 seconds, then drops sharply to room temperature in the following 1000 seconds. The static pressure increases rapidly from 1 x 10^{-4} torr to almost 10 torr during the first 500 seconds, and then gradually increases from 10 to 50 torr in the subsequent 1500 seconds, followed by a sharp increase in pressure from 50 to 760 torr between elapsed times of 2500 and 3000 seconds.

Hot Side Temperature Uniformity

An important criterion in thermal vacuum testing is to ensure uniform heating of the hot side of the entire test article at each instant of time. The uniform heating enables use of fewer thermocouples to measure temperature distributions on the hot side, and simplifies thermal analysis by employing uniform temperature boundary conditions for the computational heat transfer model of TPS. Unfortunately, quartz lamps do not have a constant longitudinal heat flux distribution. The longitudinal variation of quartz lamp arrays has been analytically studied and experimentally verified for a single lamp by Turner and Ash.[4] Johnson has also experimentally investigated the longitudinal variation of the heat flux from quartz lamp arrays.[5] He has shown that although the heat flux varies by less than 20% over most of the array, there is a significant drop-off, on the order of 50%, along the outer edges. Several techniques can be utilized either separately or in conjunction with each other to compensate for this non-uniformity. These include using a lamp array with a planar area larger than the test article, employing reflectors along the edges of the test article (between the test article and lamp array), and using additional lamps along the edges of the test article. The quartz lamp array in this study utilizes a planar area larger than the test article to achieve uniform heating of the test article.

Back Side Boundary Condition

Simulating the back side boundary condition for TPS transient testing is ambiguous and complicated. The goal of TPS design is to ensure that the temperature of the structure adjacent to the TPS backside (termed the "backside structure") doesn't exceed a critical design value throughout re-entry. The actual back side structure receives heat from the TPS, and transfers heat to a large reservoir at ambient temperature inside the aerospace vehicle. Ko, et al.,[6] have numerically simulated heat transfer through Space Shuttle Orbiter tiles into the wing box structure and have compared their results with actual measurements on the Space Shuttle. They have found that the usual assumption of adiabatic boundary condition on the back side structure is conservative. The back side structure adjacent to the TPS loses heat through internal radiation and natural convection, but the exact formulation of the heat losses from the backside structure is not trivial.

In typical numerical simulations, the back side structure is assumed to be insulated, however, experimental simulation of an insulated boundary condition is impossible. All insulations conduct heat, but more importantly, their specific heat capacity causes a portion of the impinging heat to be absorbed and stored by the insulation. In the present thermal vacuum facility, two different types of back side boundary conditions can be implemented based on the research objectives. Both require use of a base plate separated from the back side structure by a user-defined distance, L, as shown schematically in Figure 4. This space between the base plate and back side structure is filled with an insulation of user defined density and thermal insulation performance. The base plate's temperature can be allowed to float throughout the test to simulate an adiabatic boundary condition, or it can be actively controlled to simulate the actual flight boundary conditions as observed by Ko.[6] In either case, the measured base plate temperature should be used as the actual boundary condition in the computational heat transfer model for simulating the experiments, and the base plate and the insulation used between the base plate and the back side structure should be included in the computational heat transfer model.

Description of Experimental Facility

A brief description of the overall experimental facility is provided. The vacuum chamber, test article, heating array, the overall assembly, and the pressure and temperature control systems are described.

Vacuum Chamber Description

The facility vacuum chamber is cylindrical with dimensions of 54 in. long by 48 in. diameter. One end is comprised of a hinged door. The main structure is made of stainless steel, while the entire interior is lined with a thin aluminum shroud. Depending on the test temperatures and duration, it may be necessary to cool the shroud to prevent damage due to overheating. The shroud is formed to fit the shape of the chamber with hollow channels connected in the form of a manifold to conduct a cooling medium. The cooling medium can be compressed air, gaseous nitrogen or liquid nitrogen. Maximum temperatures on the shroud for the temperature profile used in this study did not exceed 350°F without cooling. There are front to back rails on each side of the chamber, which serve as supports for the combined lamp bank/test article assembly.

The chamber is equipped with feed-through fittings and connectors for instrumentation, power and gas. Power feed-throughs are rated at 200 amperes three- phase. Instrumentation feed-throughs can accommodate 150 type "T" or "K" thermocouples. A rotary vacuum pump rated at 100 ft^3/min. is used to achieve rough vacuum down to 1×10^{-2} torr. For tests requiring lower pressures a helium cooled cryo-pump can be used to achieve pressures as low as 5×10^{-6} torr. In order to ensure continuous pressure measurements over the range of high vacuum to atmosphere three types of gages are used. A capacitance gage is used between atmospheric pressure and 10 torr. A Pirani gage is used between 10 and 5×10^{-3} torr, and an ionization gage is used below 5×10^{-3} torr. The crossover between these gages is automatic.

Test Assembly

The test assembly includes the aluminum base plate, the test article, the quartz lamp array, the supporting structure, and the heat shield enclosure. A photograph of the test assembly without the heat shield enclosure, prior to installation in the vacuum chamber, is shown in Figure 5. The aluminum base plate, 50×45 in. and 0.25 in. thick, is supported by the previously described rails in the vacuum chamber. In addition to its' function in simulating the backside boundary condition, the base plate is used as a platform for the test article, the lamp array, and the heat shield enclosure.

The test article used in this investigation is an Inconel honeycomb panel resting on a Saffil® insulation layer as shown in Figure 5. The Inconel honeycomb panel was 18 in. wide, 36 in. long and 0.25 in. thick. The honeycomb panel was instrumented with 23 metal-sheathed type K thermocouples. A photograph of the Inconel honeycomb panel with its installed thermocouples is shown in Figure 6. A schematic of the layout of the thermocouples on the Inconel honeycomb panel is shown in Figure 7. The spatial locations of the thermocouples on the panel are provided in Table 1. One thermocouple in the central region (designated as Thermocouple 9) is used for feedback control for the radiant heating system. The Saffil® fibrous insulation layer was $18 \times 36 \times 1.75$ in. with a density of 1.5 lb/ft^3. Refractory fiber ceramic board spacers, 1×1 in. and 1.75 in. thick are used at the four corners of the test article to maintain a constant thickness of Saffil® insulation. The thermal response of the test panel at the four corners is dominated by the rigid ceramic board spacers, because the spacers have a much higher density (16 lb/ft^3) and thermal conductivity than the Saffil® fibrous insulation.

A custom quartz lamp heater array has been fabricated to obtain uniform heating and quick system response at test temperatures. The heater array consists of quartz lamps, an un-cooled, polished stainless steel reflector, high-density lamp holders, and copper buss bars. The array is powered by a phase angle-fired, SCR (silicon control rectifier) power controller and a 240 VAC, three-phase transformer. The transformer is configured for a maximum voltage of 220 VAC to avoid electrical arcing encountered at higher voltages in low-pressure environments. 2500T3/CL quartz lamps with a lighted length of 25 in, rated at 2500 W/460-500 VAC, are used to provide a 3.5 in. overhang along the sides of the 18 in. wide test article. The array consists of 84 lamps spaced 0.5 in. apart, providing a three inch overhang at the ends of the 36 in. long test article. A rule of thumb for quartz lamp heater design requires a stand-off distance of four times bulb spacing to achieve uniform heat density, therefore, the distance between the lamp array and test article is set at two inches.

The lamp array uses a polished, un-cooled stainless steel sheet reflector. Stainless steel has been successfully used as a reflector for steady-state specimen temperatures to 2000°F in air.[7] Its' high melting point and structural stability make it an ideal un-cooled reflector. Because of the high efficiency of radiant heating in vacuum, stainless steel could safely be used as an un-cooled reflector without the complexity of active cooling. The panel side of the reflector has been brightened to a 63 surface finish by polishing with emery cloth to increase its reflectance.

The lamps are attached to the reflector with high-density, T3 quartz lamp support assemblies. This rugged design has been a staple of custom quartz lamp fabrication since the 1950's. The lamps are wired in parallel, in groups of 28, to 1×0.25 in. copper buss bars. The lamp pigtails are connected to the busses with high temperature stainless steel ring terminals and screws.

Two longitudinal stiffening beams are fastened to the stainless steel reflector plate in order to counteract its tendency to warp under heat, as shown in Figure 8. This assembly is held together by threaded rods that are easily adjusted to accommodate test articles of varying thickness and for varying the spacing of the lamps from the test article. The lamp array can be supported at a 45-degree angle for test article access. Heat shield components, made from 0.031 in. thick stainless steel are installed to shield the inside of the chamber from stray radiation. Appropriate notches are cut in the heat shield for the instrumentation wires and the lamp power cables. A photograph of the overall setup with partial installation of the heat shield enclosure is shown in Figure 9. All areas on the base plate that are within view of the lamps are covered with insulation before the structure is tilted back down to the operating position. One inch thick ceramic board insulation is used as a liner for the heat shield. Depending on the test temperature, additional Saffil® insulation blankets may be installed on the outside of the heat shields to further isolate the chamber shrouds from the heat. Because it was difficult to work on the test article within the confines of the chamber, the test assembly is built up prior to installing in the chamber. The test assembly is then placed in the chamber with a forklift. A Photograph of the test assembly after installation in the vacuum chamber is shown in Figure 10. Additional Saffil® insulation located on top of the test assembly is shown in the photograph.

Temperature and Pressure Control

Pressure and temperature control are accomplished using a custom written control program running on a personal computer. PID (proportional, integral, derivative) control is used for the temperature and proportional control is used for the pressure. A plug-in interface board provides the necessary analog input, analog and digital outputs. The voltage of the control thermocouple located in the center of the test article is read by the analog input and then converted to temperature. The analog output is used to control the SCR power controller, and the digital outputs are used to control the pressure.

A data file providing the target re-entry profile temperatures and pressures as a function of elapsed time is required. The profile used in the present study has 98 entries, with each entry representing one set of data points (elapsed time, temperature, pressure). The file is preprocessed to calculate the temperature and pressure rates of change and a new file is created with elapsed time, rate of change, target

temperature and pressure. This file serves as the input to the control program. When the test is started, the set point is initialized at the actual temperature. A new set point is continually calculated based on the target temperature, rate and the time. When the calculated set point reaches the target temperature, the next target temperature and rate of change are retrieved from the file until all of the file entries are utilized. The set point is constantly being compared to the actual temperature to calculate an error term that is processed by the PID algorithm to derive the proper control output to send to the SCR power controller. The voltage analog output is fed through a voltage-current converter to produce the 4 – 20 milliamp current output required by the power controller. This circuit has a two second time constant to compensate for the high initial current draw resulting from the low, room temperature electrical resistance of the tungsten heating elements. The set point and actual temperature are plotted in real time during the test.

Re-entry pressure is simulated by bleeding nitrogen into the chamber, monotonically changing from a low to high pressure. Two separate, pre-adjusted needle valves, each in series with an open/closed solenoid valve are used for changing pressure in either the low or high-pressure regime. Two, 0 - 5 volt digital outputs from the pressure control system energize the solid-state relays that operate the 120 VAC solenoid valves. Nitrogen is bled into the chamber by the needle valves. The proportional control program compares the pressure set point for each file entry with the actual pressure. If the error is greater than five percent the appropriate solenoid valve is opened continuously. If the error is below five percent the open time is set proportional to the error, allowing the pressure to creep up on the set point without overshoot. The pressure set point and actual pressure are plotted in real time to ascertain proper performance.

Prior to running a test the chamber must be thoroughly rough-pumped. This is primarily to remove water that has been adsorbed onto the chamber walls and other components or absorbed into the porous insulation boards and bats. Failure to remove this water will result in rapid out-gassing during heat up which results in a pressure rise. The resulting pressure rise may exceed the test pressure profile, resulting in poor pressure control. Rough pumping is continued until a closed valve pressure rise of less than 0.01 torr per hour was observed.

Results and Discussion

Two tests were performed. The overall results were repeatable, therefore, only the results of one test are described. The comparison of temporal variation of actual static pressure in the vacuum chamber with the desired re-entry profile is shown in Figure 11. The pressure in the vacuum chamber could not be controlled accurately below 0.01 torr for the transient tests, resulting in a difference between chamber pressure and the desired re-entry profile for elapsed times below 300 seconds. The pressure in the chamber followed the desired pressure closely between elapsed times of 300 and 2400 seconds. Within this time period the average percent difference between measured and re-entry pressures was –1.6% with a standard deviation of ±7.4%. The measured pressures were slightly different from the desired re-entry profile after an elapsed time of 2400 seconds. Within this time period the average percent difference between measured and re-entry pressures was –10.3% with a standard deviation of ± 15.3%.

The comparison of the hot side temperature, measured by the control thermocouple on the Inconel honeycomb panel, and the re-entry profile is shown in Figure 12. The control temperature closely followed the re-entry profile during the initial heating phase, (0-500 sec.). Within this time period the average percent difference between measured and re-entry temperatures was –1.7% with a standard deviation of ± 0.4%. After 500 seconds the measured temperature could not follow the re-entry profile due to the PID controller characteristics, but eventually caught up with the re-entry profile around 1250 seconds. In the time period between 500 and 1400 seconds, the average percent difference between measured and re-entry temperature was –3.0% with a standard deviation of ± 2.9%. After 1400 seconds, with the exception of two short duration heat pulses, there was a rapid decrease in the re-entry profile due

to high convective cooling at lower altitudes. Because the current thermal vacuum setup was not equipped with active cooling, implementing such a high cooling rate was not possible. The measured temperatures exceeded the desired profile by different margins over this time interval. This time span can be divided into two different regions. Between 1400 and 2000 seconds, the average percent difference between measured and re-entry temperature was 7.6% with a standard deviation of ± 6.5%. After 2000 seconds, the deviation between the measured and re-entry profile grew with time. As discussed previously, if TPS thermal vacuum testing can not duplicate the re-entry profile exactly, it is still useful to provide simulations that will be used for validation of computational heat transfer models of TPS. The validated computational models can then be used to predict the TPS performance under the exact re-entry conditions. Given that the re-entry profile could be duplicated to within 7.6% up to 2000 seconds, the simulation capability was deemed as acceptable.

To investigate temperature uniformity of the test panel throughout the test, the statistical variations of temperature measurements over different panel areas were studied. The temporal variation of the standard deviation of the thermocouples was calculated for three zones. Zone one included all the thermocouples on the panel, while the second and third zones included all the thermocouples within 17 in. and 10 in. radii of the panel center, respectively. Zone three consisted of thermocouple numbers 3, 4, 5, 6, 7, 8, 10, 11, 12, 13, 14, and 15 as shown in Figure 7. Zone two consisted of all the thermocouples in zone three plus thermocouple numbers 16, 17, 18, 19, and 21. The variation of the standard deviation of the thermocouples in each zone with elapsed time is shown in Figure 13. During the initial heating phase (0 to 500 sec.), the standard deviation of the temperatures in the three zones approached 50-70°F. After the initial heating phase, the standard deviation of the temperatures in the three zones generally decreased with increasing test time. In the time period between 500 and 1500 seconds, when the panel temperature is maintained around 1800°F, the standard deviations of temperatures in the three zones varied between 15 and 33°F. After 1500 seconds, the standard deviations varied between 8 and 28°F. Ignoring the data for the initial heating phase, the uniformity of temperatures improved as the area being considered decreased. It is believed that this non-uniformity was caused by inherent non-uniformities in quartz lamp arrays, and the influence of thermal boundary conditions at the edges of the panel. In order to gain an insight into the relative magnitude of these non-uniformities with respect to actual panel temperatures, the ratios of the temperature standard deviation with respect to the average temperature in each zone were calculated and plotted in Figure 14. The temperature non-uniformities reached 12 to 16 percent during the initial heating phase, but were generally less than 2 percent after an elapsed time of 500 seconds.

To further investigate the temperature uniformity of the panel, the temporal variations of the temperature difference between various thermocouples and the thermocouple in the center of the panel are shown in Figure 15. The figure includes data for thermocouples 14, 16, 21, and 23. As shown in Figure 7 thermocouple 23 was at one corner of the panel, while thermocouples 16 and 21 were 1 in. away from the panel edge, while thermocouple 14 was halfway between the center thermocouple and thermocouple 21. All the thermocouples read higher than the center thermocouple, by as much as 150°F, during the initial heating phase (0 to 500 sec.). After 500 seconds, the thermocouples generally read lower than the center thermocouple, with the maximum deviation of -100°F at thermocouple 23. The corner thermocouple (23) had the highest deviation, while the deviation of the two edge thermocouples (16 and 21) were comparable, with thermocouple 14 having the lowest deviation (-25°F). A contour plot of temperatures across the upper right quadrant of the panel ($18 \leq x \leq 36$, $9 \leq y \leq 18$) at elapsed time of 1200 seconds is shown Figure 16.

The uniformity of the present system can be compared to a similar Radiant Heat Test Facility at Johnson Space Center. This facility can be used to simulate the thermal and static pressure environments for general spacecraft thermal protection systems during the ascent, orbit and entry phases. It uses a radiant heater consisting of electrically heated graphite elements enclosed in a nitrogen purged fixture box. This facility has previously been used for testing a two-panel array of a superalloy honeycomb prepackaged metallic TPS, with each panel being 12×12 in.[8] In these tests nine thermocouples were installed on the panel's hot side, with four of the thermocouples located close to the corners of the test

article. At an elapsed time of 620 sec. the average panel temperature was 1787°F, with a standard deviation of 91.1°F.[8] At this instant of time, the four corner thermocouples varied from the center thermocouple by 160-220°F.[8] It should be noted that the heating profile used by Gorton, at al,[8] was representative of a Space Shuttle Orbiter re-entry and is different from the heating profile used in this study. The comparable time duration for the present test was 1200 seconds, at which time the panel temperature was 1800°F with a standard deviation of 30°F, with maximum temperature difference from panel's center being 100°F. It should also be noted that the TPS geometry tested by Gorton, et al,[8] was more complex than the simple Inconel honeycomb panel used for this investigation, and the temperature non-uniformities can not be directly compared.

The overall results indicated that the present thermal vacuum heating system was capable of providing uniform test specimen temperature with variations of 16% during the initial heating phase, and 2 % percent during the remainder of the test. The system was capable of following the desired pressure profile very closely, and managed to follow the required temperature profile closely for up to 2000 seconds in the profile.

Concluding Remarks

A thermal vacuum facility for testing launch vehicle thermal protection systems by subjecting them to transient thermal conditions simulating re-entry aerodynamic heating was developed and evaluated. The facility can be used for testing specimens as large as 18×36 in. An un-cooled, 25 in. wide, 42 in. long quartz lamp array operating on a maximum voltage of 220 VAC is used to radiantly heat the specimens. The test set-up is housed in a 54 in. long, 48 in. diameter vacuum chamber that can use either nitrogen or air as the working gas. Temperature and pressure control are accomplished using a custom written control program running on a personal computer. The facility can be reconfigured to accommodate test articles of various sizes. Overall facility performance was evaluated by subjecting an 18×36 in. Inconel honeycomb panel, instrumented with 23 metal-sheathed thermocouples, to a typical re-entry pressure and surface temperature profile (3200 seconds long). For most of the test duration, the average difference between the measured and desired pressures was 1.6 % of reading with a standard deviation of ±7.4%, while the average difference between measured and desired temperatures was 7.6% of reading with a standard deviation of ±6.5%. The temperature non-uniformity across the panel was 12% percent during the initial heating phase (t ≤500 sec.), and less than 2% during the remainder of the test. The maximum temperature difference, between the temperatures measured anywhere on the panel and the panel's center, was 150°F during the initial heating phase (t ≤500 sec.) and 100°F during the rest of the test.

List of References

1. Blosser, M.; Chen, R., Schmidt, I., Dorsey, J.; Poteet, C., and Bird, K.: "Advanced Metallic Thermal Protection System Development," AIAA Paper 2002-504, January 2002.

2. Thornton, E.A., *Thermal Structures for Aerospace Applications*, American Institute of Aeronautics and Astronautics, Reston, VA, 1996.

3. Blosser, M.L., " Advanced Thermal Protection Systems for Reusable Launch Vehicles," PhD Dissertation, University of Virginia, May 2000.

4. Turner, T.L., and Ash, R.L., "Analysis of the Thermal Environment and Thermal Response Associated with Thermal-Acoustic Testing," AIAA Paper 90-0975, April, 1990.

5. Johnson, J.D., "Thermally-Induced Structural Motions of Satellite Solar Arrays," PhD Dissertation, University of Virginia, May 1999.

6. Ko, W.L., Quinn, R.D., and Gong, L., "Finite-Element Reentry Heat-Transfer Analysis of Space Shuttle Orbiter," NASA TP 2657, December 1986.

7. Berman, J.S., "Research into the Application of Radiant Heating to the Structural Testing of Aircraft at Elevated Temperatures," Wright-Patterson Air Force Base Contract Report AF 33(616)-2162, 1954.

8. Gorton, M.P., Shideler, J.L., and Webb, G.L., "Static and Aerothermal Tests of a Superalloy Honeycomb Prepackaged Thermal Protection System," NASA TP-3257, March 1993.

Thermocouple designation	x, in	y, in	Thermocouple designation	x, in	y, in
1	1	1	13	27	5
2	1	17	14	27	9
3	9	9	15	27	13
4	18	1	16	27	17
5	18	5	17	31.5	9
6	18	9	18	31.5	13
7	18	13	19	31.5	17
8	18	17	20	35	1
9	19	9	21	35	9
10	22.5	9	22	35	13
11	22.5	13	23	35	17
12	22.5	17			

Table 1. Spatial location of thermocouples on Inconel honeycomb panel
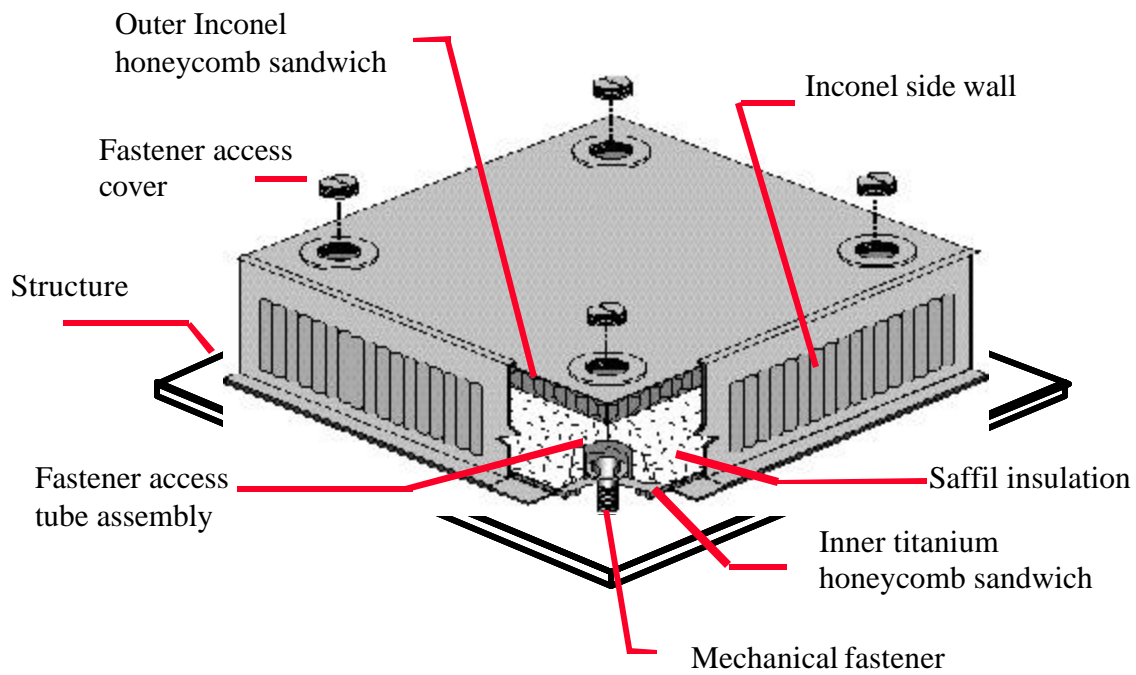
Figure 1. Schematic of a typical metallic thermal protection system.
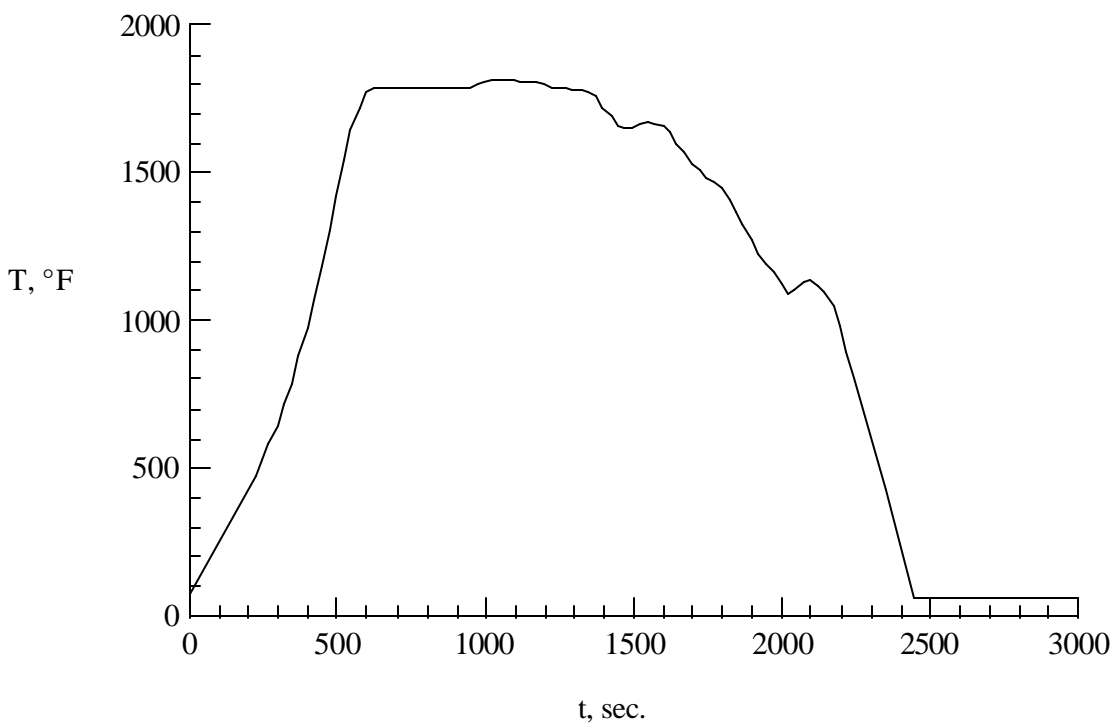
Figure 2. Typical re-entry surface temperature profile.
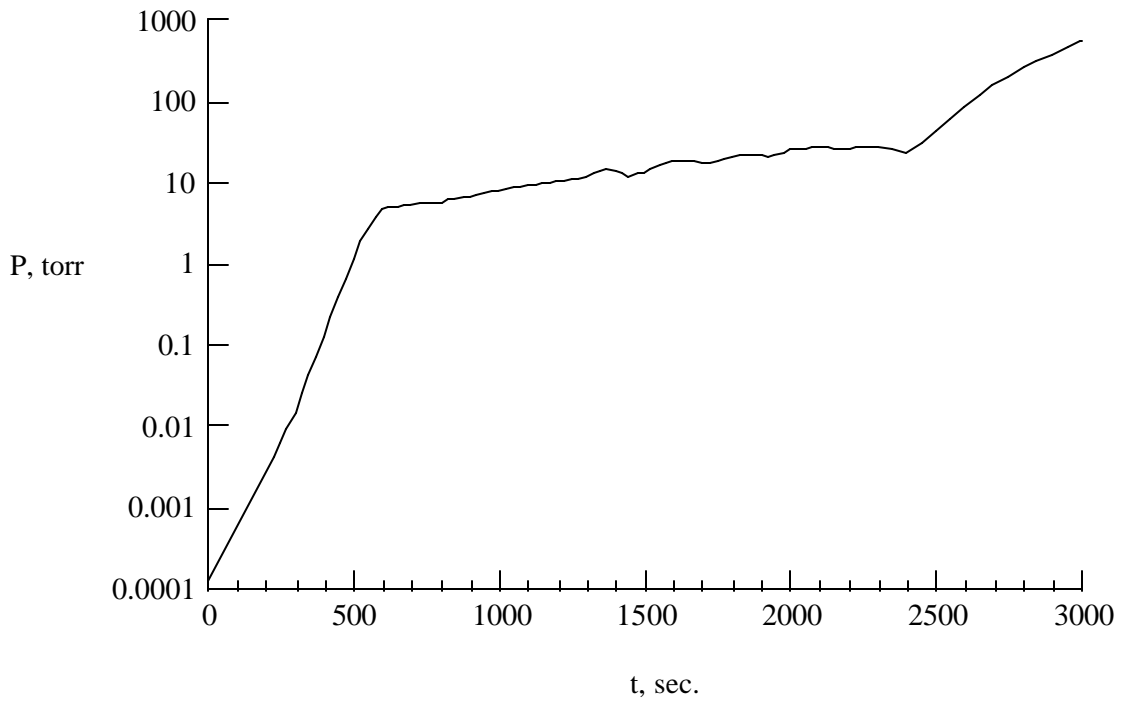
Figure 3. Typical re-entry pressure profile.
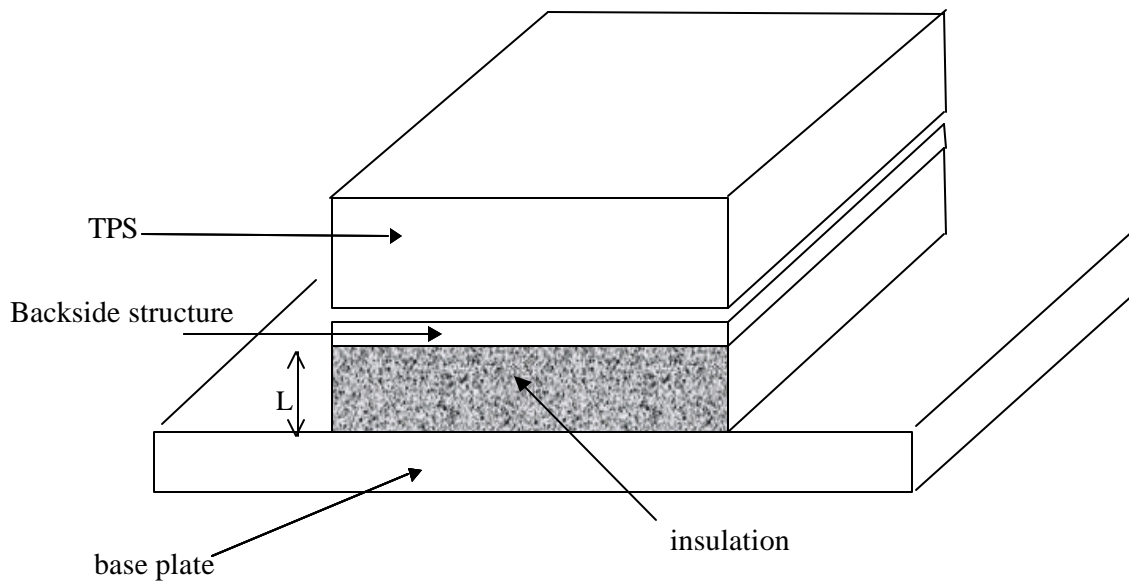
Figure 4. Schematic of test article setup in vacuum chamber.
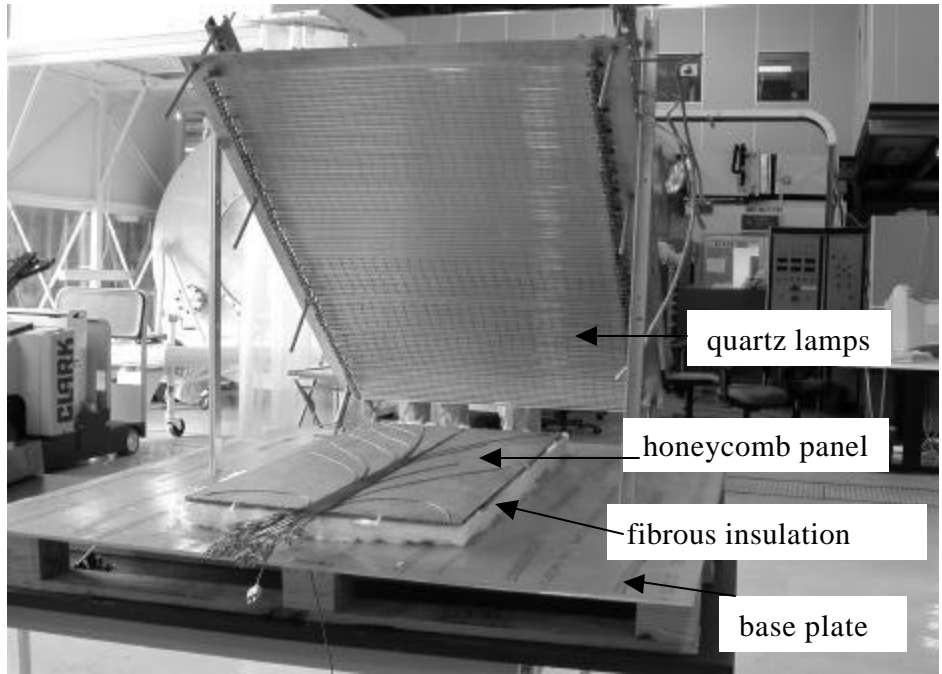
Figure 5. Lamp bank in tilted position for test article access.
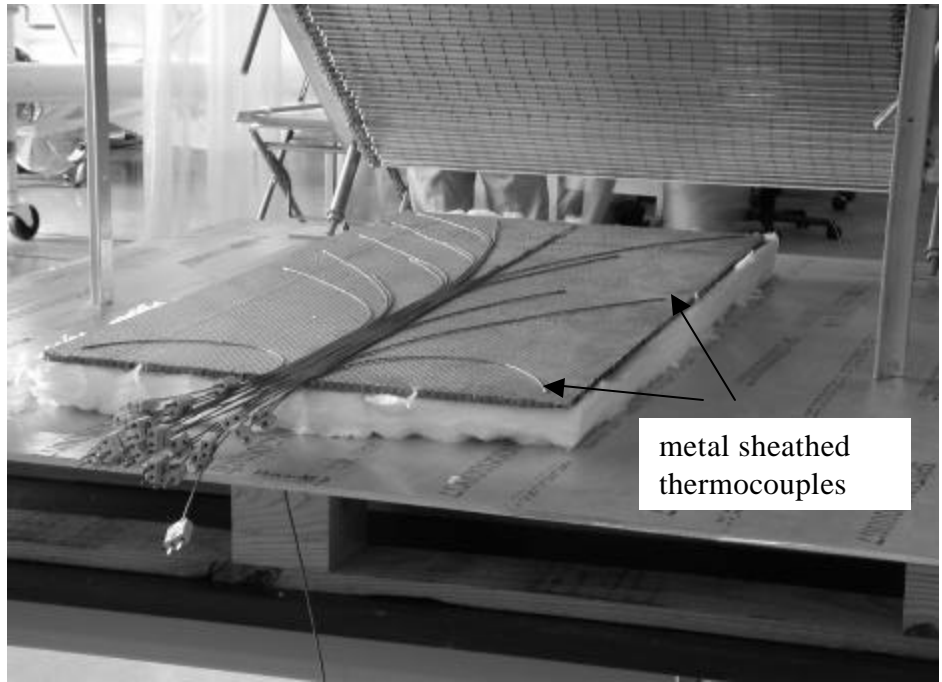
Figure 6. Photograph of the Inconel honeycomb panel and its measurement and control thermocouples.
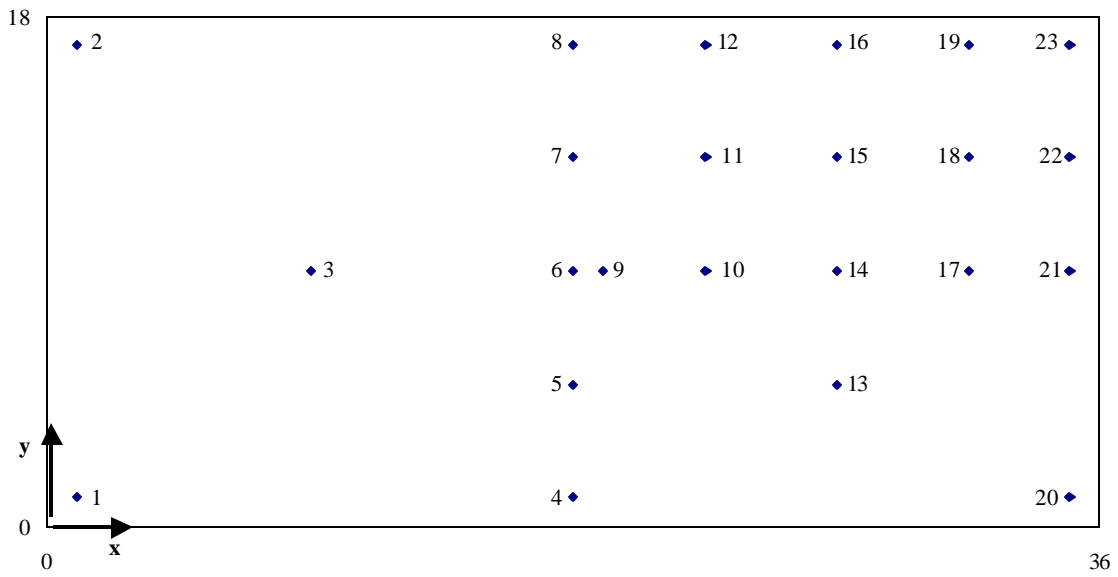
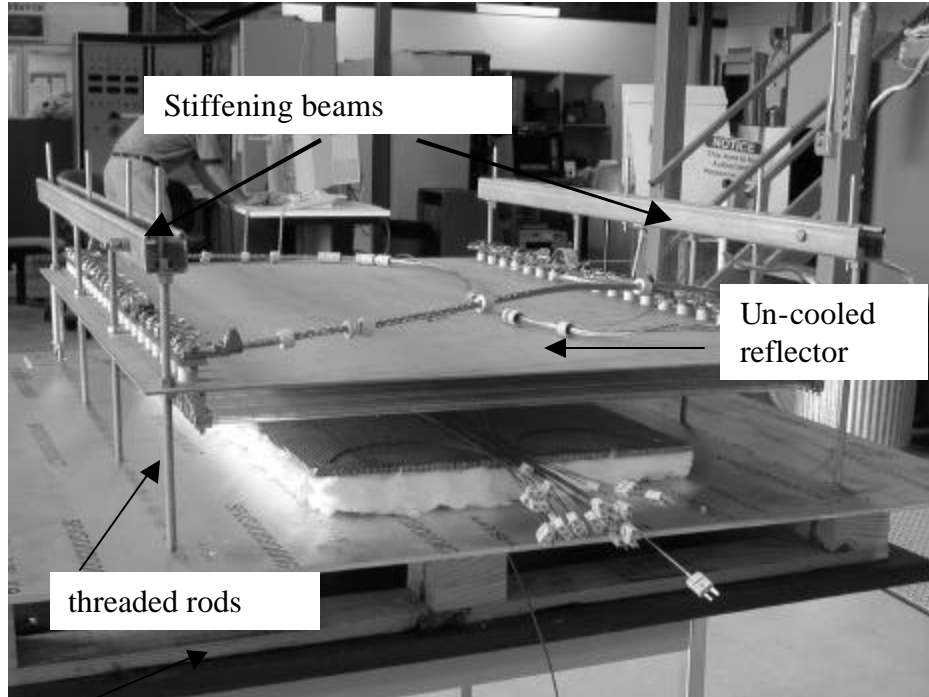Figure 7. Schematic of thermocouple layout on the Inconel honeycomb panel (9 is the control thermocouple).

Figure 8. Support structure for quartz lamp array.
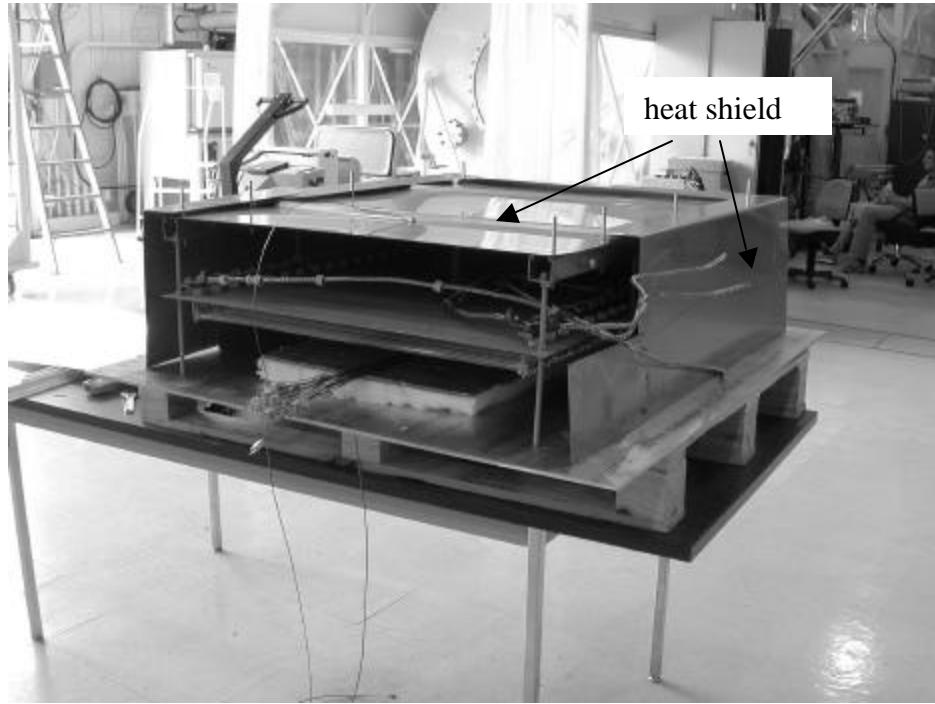
Figure 9. Photograph of test assembly with partial installation of heat shields.
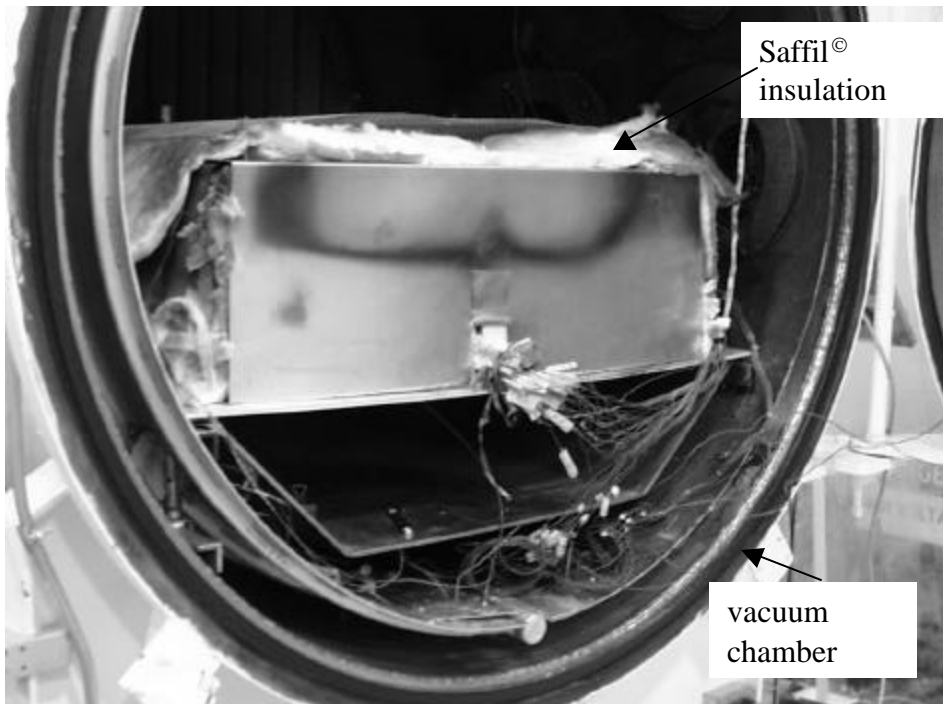
Figure 10. Test assembly in the vacuum chamber.
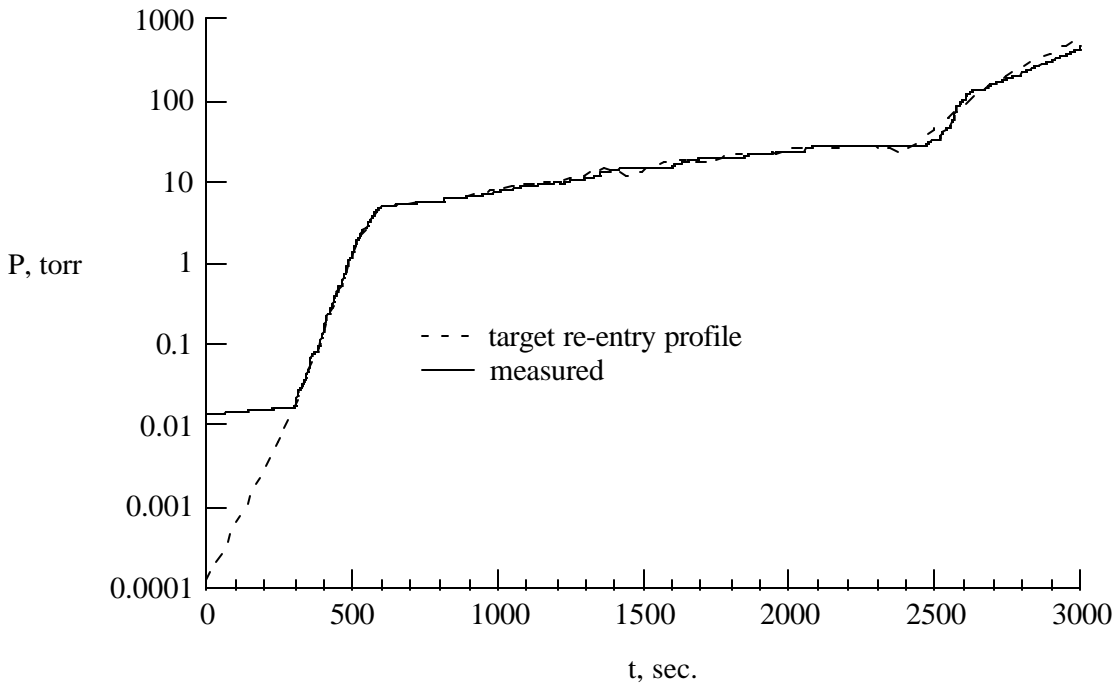
Figure 11. Comparison of measured and target re-entry pressure profiles as a function of re-entry elapsed time.
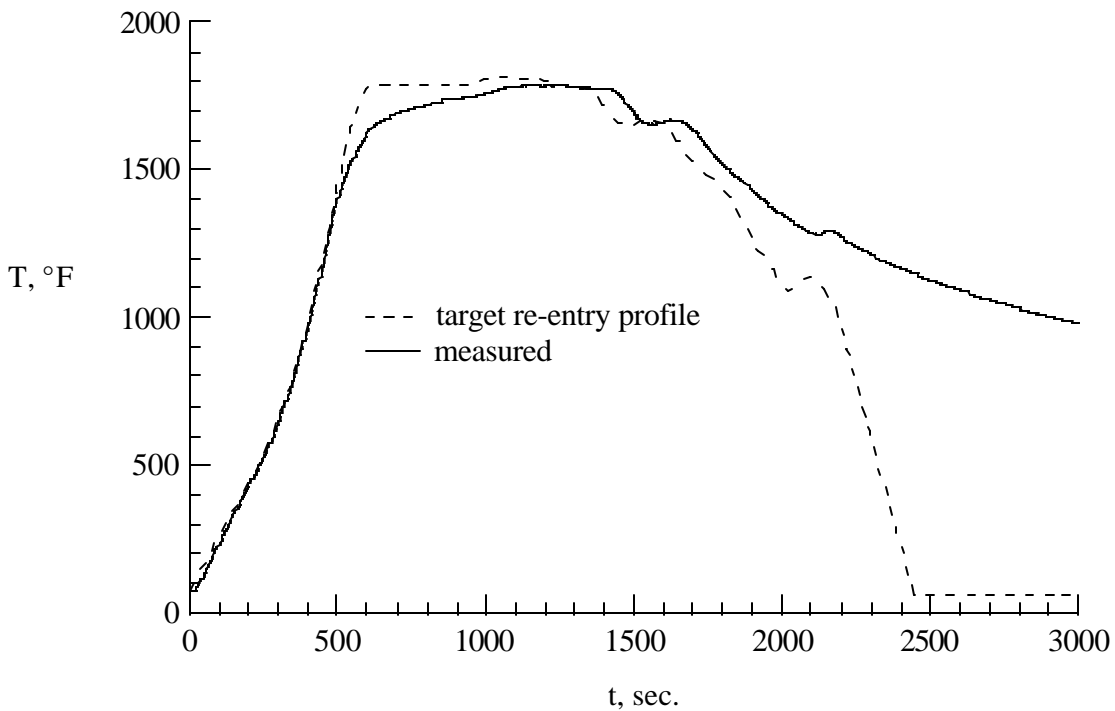
Figure 12. Comparison of measured and target re-entry surface temperature profiles as a function of re-entry elapsed time.
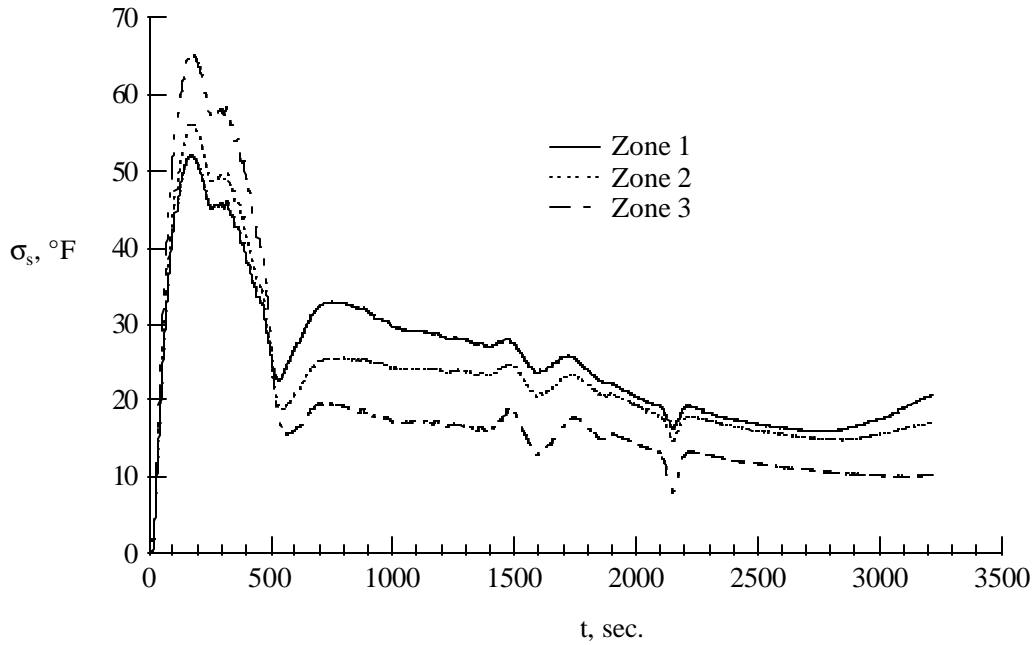
Figure 13. Temporal variation of standard deviation of temperature in three zones.
(Zone 1: all thermocouples, Zone 2: thermocouples within 17 in. radius of panel center, Zone 3: thermocouples within 10 in. radius of panel center)
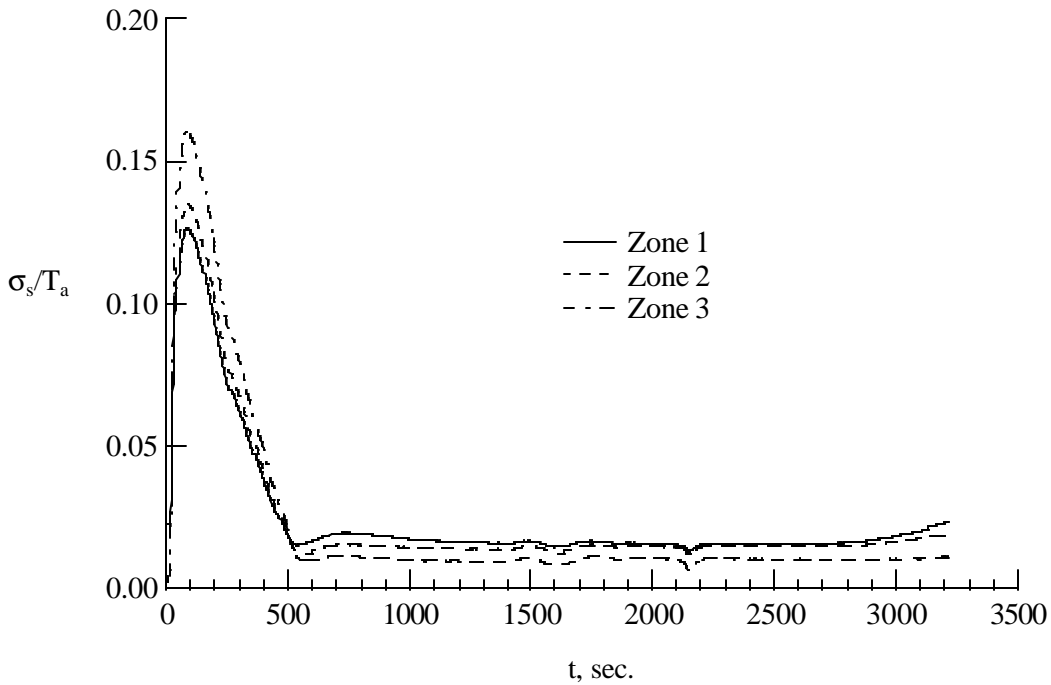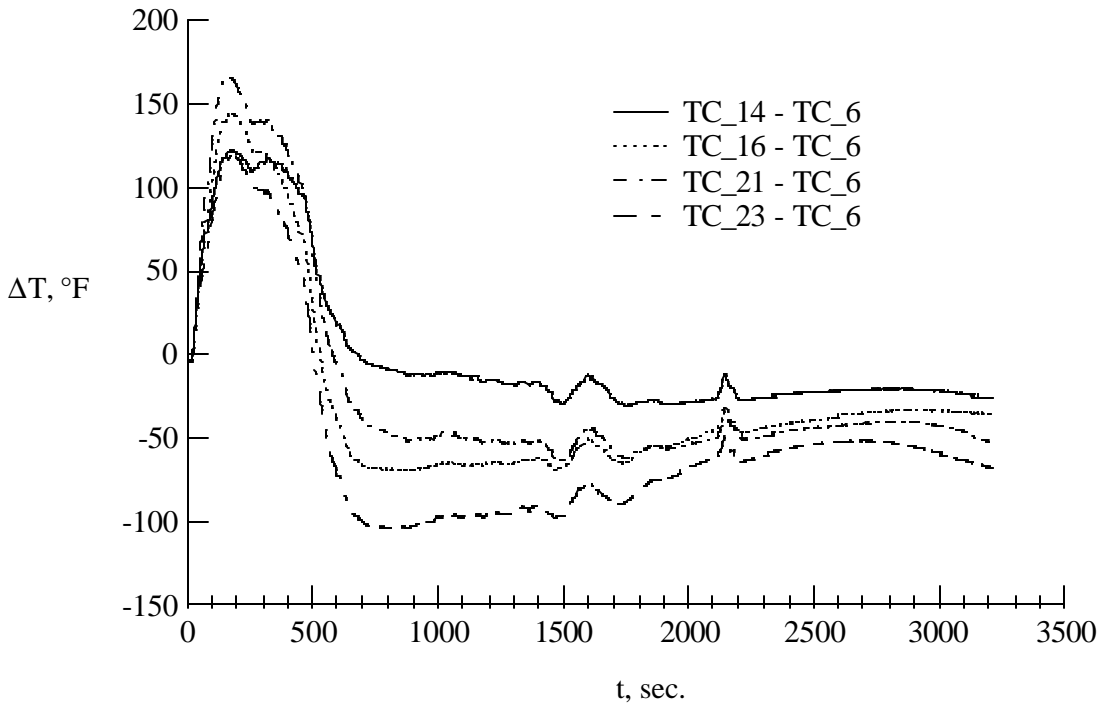

Figure 14. Temporal variation of the ratio of standard deviation to average temperature for three zones. (Zone 1: all thermocouples, Zone 2: thermocouples within 17 in. radius of panel center, Zone 3: thermocouples within 10 in. radius of panel center)

16

Figure 15. Temporal variation of temperature difference between listed thermocouples and panel center's thermocouple.
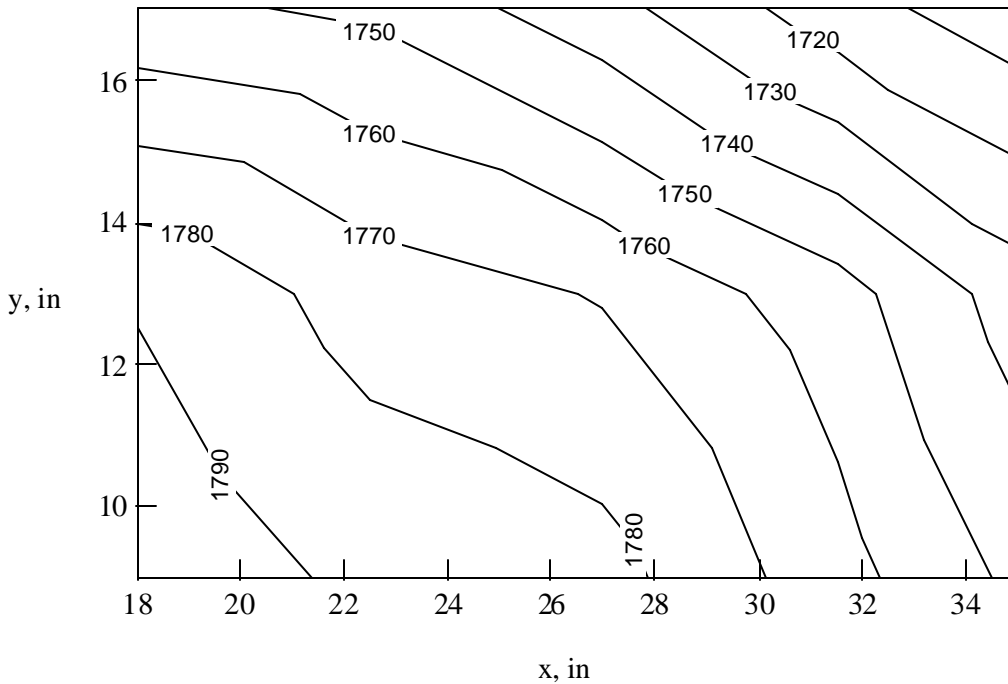

Figure 16. Contour plot of temperature distribution in the upper right hand quadrant of plate at test elapsed time of 1200 sec.

REPORT DOCUMENTATION PAGE

1. AGENCY USE ONLY (*Leave blank*)	2. REPORT DATE June 2002	3. REPORT TYPE AND DATES COVERED Technical Memorandum

4. TITLE AND SUBTITLE
Thermal Vacuum Facility for Testing Thermal Protection Systems

5. FUNDING NUMBERS
721-21-51-05

6. AUTHOR(S)
Kamran Daryabeigi, Jeffrey R. Knutson, and Joseph G. Sikora

7. PERFORMING ORGANIZATION NAME(S) AND ADDRESS(ES)

NASA Langley Research Center
Hampton, VA 23681-2199

8. PERFORMING ORGANIZATION REPORT NUMBER

L-18163

9. SPONSORING/MONITORING AGENCY NAME(S) AND ADDRESS(ES)

National Aeronautics and Space Administration
Washington, DC 20546-0001

10. SPONSORING/MONITORING AGENCY REPORT NUMBER

NASA/TM-2002-211734

11. SUPPLEMENTARY NOTES

12a. DISTRIBUTION/AVAILABILITY STATEMENT
Unclassified-Unlimited
Subject Category 34   Distribution: Standard
Availability: NASA CASI (301) 621-0390

12b. DISTRIBUTION CODE

13. ABSTRACT (*Maximum 200 words*)
A thermal vacuum facility for testing launch vehicle thermal protection systems by subjecting them to transient thermal conditions simulating re-entry aerodynamic heating is described. Re-entry heating is simulated by controlling the test specimen surface temperature and the environmental pressure in the chamber. Design requirements for simulating re-entry conditions are briefly described. A description of the thermal vacuum facility, the quartz lamp array and the control system is provided. The facility was evaluated by subjecting an 18 by 36 in. Inconel honeycomb panel to a typical re-entry pressure and surface temperature profile. For most of the test duration, the average difference between the measured and desired pressures was 1.6% of reading with a standard deviation of $\pm 7.4\%$, while the average difference between measured and desired temperatures was 7.6% of reading with a standard deviation of $\pm 6.5\%$. The temperature non-uniformity across the panel was 12% during the initial heating phase ($t \leq 500$ sec.), and less than 2% during the remainder of the test.

14. SUBJECT TERMS
Thermal protection system, Re-entry heating, Thermal-vacuum test

15. NUMBER OF PAGES
22

16. PRICE CODE

17. SECURITY CLASSIFICATION OF REPORT Unclassified	18. SECURITY CLASSIFICATION OF THIS PAGE Unclassified	19. SECURITY CLASSIFICATION OF ABSTRACT Unclassified	20. LIMITATION OF ABSTRACT UL